Bimetallic MOFs $(H_3O)_x[Cu(MF_6)(pyrazine)_2]\cdot(4-x)H_2O$ (M = V^{4+}, x = 0; M = Ga^{3+}, x = 1): co-existence of ordered and disordered quantum spins in the V^{4+} system†

Jamie L. Manson,*[a] John A. Schlueter,[b] Kerry E. Garrett,[a] Paul A. Goddard,[c] Tom Lancaster,[d] Johannes S. Möller,‡[e] Stephen J. Blundell,[e] Andrew J. Steele,[e] Isabel Franke,[e] Francis L. Pratt,[f] John Singleton,[g] Jesper Bendix,[h] Saul H. Lapidus,[i] Marc Uhlarz,[j] Oscar Ayala-Valenzuela,[g] Ross D. McDonald,[g] Mary Gurak[g] and Christopher Baines[k]

The title compounds are bimetallic MOFs containing $[Cu(pyz)_2]^{2+}$ square lattices linked by MF_6^{n-} octahedra. In each, only the Cu^{2+} spins exhibit long-range magnetic order below 3.5 K (M = V^{4+}) and 2.6 K (M = Ga^{3+}). The V^{4+} spins remain disordered down to 0.5 K.

Low-dimensional metal–organic solids have yielded a plethora of interesting structure types that display a broad range of magnetic behaviors including bistability, slow relaxation of the magnetization, and conventional Néel order.[1] The design of such materials depends on the symmetry, size, reactivity, and stability of the building block(s) used to prepare them. A great advantage of metal–organic systems (relative to metal oxides for example) is

their general ease of synthesis and systematic tunability of physical properties by the variation of the metal ion (identity and/or oxidation state) and the organic ligands. For magnetic materials, paramagnetic building blocks are obviously important and the search for new examples with desired properties is an on-going endeavor.

Discrete perfluoro MF_6^{3-} complexes[2–4] are known for M = V^{3+}, Cr^{3+}, and Fe^{3+} whereas MF_6^{2-} is exceedingly sparse with only one example, VF_6^{2-},[5] reported to date. It would be of great interest to employ these open-shell, valence flexible, complexes as building blocks to synthesize extended structures analogous to Prussian Blues and the like.[6] Recently, it has been shown in μ-F dimers such as $[Cu_2(\mu\text{-F})(\mu\text{-L})_2](BF_4)_3$ {L = *m*-bis[bis(3,5-dimethyl-1-pyrazolyl)-methyl]benzene} that linear Cu–F–Cu bridges can support superexchange interactions as high as 450 K.[7]

Fluoride ion, with its simultaneous preference for linear bridging and for metal centers in high oxidation states, can direct the self-assembly of extended structures. Here, we report on the bimetallic $[Cu(VF_6)(pyz)_2]\cdot4H_2O$ (**1**) and $(H_3O)[Cu(GaF_6)(pyz)_2]\cdot3H_2O$ (**2**) with pyz being pyrazine. The respective VF_6^{2-} and GaF_6^{3-} building blocks were generated *in situ* from VF_4 and GaF_3 precursors in the presence of HF(aq) or aqueous NH_4HF_2.§ Their crystal structures consist of 3D metal–organic frameworks (MOFs) composed of 2D $[Cu(pyz)_2]^{2+}$ square sheets bridged by paramagnetic VF_6^{2-} (**1**) or diamagnetic GaF_6^{3-} (**2**) moieties. Study of their magnetic property reveals that only the Cu^{2+} moments undergo long-range magnetic order (LRO) in both compounds. Thus, we propose that the S = 1/2 V^{4+} sites in **1** facilitate the interlayer exchange interaction but themselves remain disordered down to at least 0.5 K.

The structures of **1** and **2** were determined at 100 K using single crystal X-ray diffraction methods.[8] Both crystallize in the tetragonal space group *P4/nbm* and have similar unit cell parameters. The Cu^{2+} ion occupies a 422 symmetry site whereas V^{4+}/Ga^{3+} sites reside on inversion centers. Each Cu^{2+} ion is ligated to four N-donor atoms from different pyrazine ligands at

[a] Department of Chemistry and Biochemistry, Eastern Washington University, Cheney, WA 99004, USA. E-mail: jmanson@ewu.edu

[b] Materials Science Division, Argonne National Laboratory, Argonne, IL 60439, USA

[c] Department of Physics, University of Warwick, Coventry CV4 7AL, UK

[d] Center for Materials Physics, Durham University, Durham DH1 3LE, UK

[e] Clarendon Laboratory, Department of Physics, University of Oxford, Oxford OX1 3PU, UK

[f] ISIS Pulsed-Muon Facility, STFC Rutherford Appleton Laboratory, Chilton, Oxfordshire OX11 0QX, UK

[g] National High Magnetic Field Laboratory, Los Alamos National Laboratory, Los Alamos, NM 87545, USA

[h] Department of Chemistry, University of Copenhagen, Copenhagen DK-2100, Denmark

[i] X-ray Science Division, Advanced Photon Source, Argonne National Laboratory, Lemont IL 60439, USA

[j] Hochfeld-Magnetlabor Dresden (HLD-EMFL), Helmholtz-Zentrum Dresden Rossendorf, DE-01314, Dresden, Germany

[k] Laboratory for Muon-Spin Spectroscopy, Paul Scherrer Institut, CH-5232 Villigen PSI, Switzerland

† Electronic supplementary information (ESI) available: CIFs for $[Cu(VF_6)(pyz)_2]\cdot4H_2O$ and $(H_3O)[Cu(GaF_6)(pyz)_2]\cdot3H_2O$ at 100 K. CCDC 1494074 and 1494075. Thermal ellipsoid plots, atom labelling scheme and ESR data. Data presented in this paper resulting from the UK effort will be made available at http://wrap.warwick.ac.uk/81878. For ESI and crystallographic data in CIF or other electronic format see DOI: 10.1039/c6cc05873f

‡ Current address: Neutron Scattering and Magnetism, Laboratory for Solid State Physics, ETH Zurich, Zurich, Switzerland.

distances of 2.050(1) Å (**1**) and 2.045(1) Å (**2**) while the axial Cu–F1 distances are longer at 2.238(2) Å (**1**) and 2.236(1) Å (**2**). The local geometry about the CuN_4F_2 core is very similar for **1**, **2**, and $[Cu(HF_2)(pyz)_2]BF_4$.[9] In **1**, the V^{4+} center is coordinated to six different F^- anions at distances of 1.870(2) (2×) and 1.927(1) Å (4×) for V–F1 and V–F2, respectively. Thus, within experimental error the VF_6^{2-} ion can be described as isotropic; the GaF_6^{3-} anion in **2** behaves similarly.

In **1** and **2**, pyz ligands connect Cu^{2+} centers to form 2D square sheets [Cu···Cu = 6.882(1) Å for **1** and 6.868(1) for **2**] within the *ab*-plane while bridging VF_6^{2-}/GaF_6^{3-} anions link the sheets together [Cu···V = 4.108(1) Å for **1**; Cu···Ga = 4.121(1) Å for **2**] to afford Cu–F–M–F–Cu chains along the *c*-axis. The result is the 3D polymeric framework depicted in Fig. 1. The 4-fold rotational symmetry of the Cu^{2+} site imposes a propeller-like disposition of the pyz ligands, giving a tilt angle of 62.84(6)° (**1**) and 63.39(6)° (**2**) relative to the CuN_4 equatorial plane. Both angles are greater/less than the corresponding angles of 59.4(2)/81.4(1)° found in $[Cu(HF_2)(pyz)_2]BF_4$ and its SbF_6-analog.[9,10] The MF_4 plane (that contain F2) within the MF_6^{n-} core is rotated about the *c*-axis by 45° relative to CuN_4 thus, all MF_6^{n-} octahedra along the *c*-direction share identical configurations. Waters of crystallization occupy each pore and form hydrogen bonds with terminal F atoms from MF_6^{n-} octahedra [(**1**): H1A–F2 = 1.86(1) Å, O1–H1A–F2 = 176(2)°; (**2**): H1–F1 = 1.85(1) Å, O1–H1–F1 = 178(2)°]. For **2**, one out of every four H_2O's is a charge-compensating H_3O^+ cation, and because of the 4-fold symmetry of those sites, the proton is positionally disordered. Electron-density difference maps support this conclusion.

The magnetic susceptibility $\chi(T)$ obtained for polycrystalline samples of **1** and **2** between 2 and 300 K are shown collectively
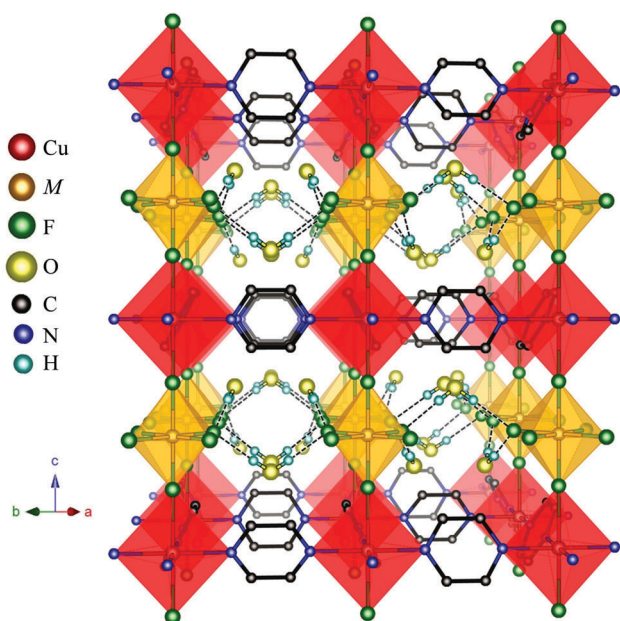

Fig. 1 Polyhedral rendition of the metal–organic framework (MOF) for $(H_3O)_x[Cu(MF_6)(pyz)_2]\cdot(4-x)H_2O$ {(**1**) M = V, x = 0; (**2**) M = Ga, x = 1}. The strong O–H···F hydrogen bonds are delineated by dashed lines. Pyz H-atoms are omitted for clarity.
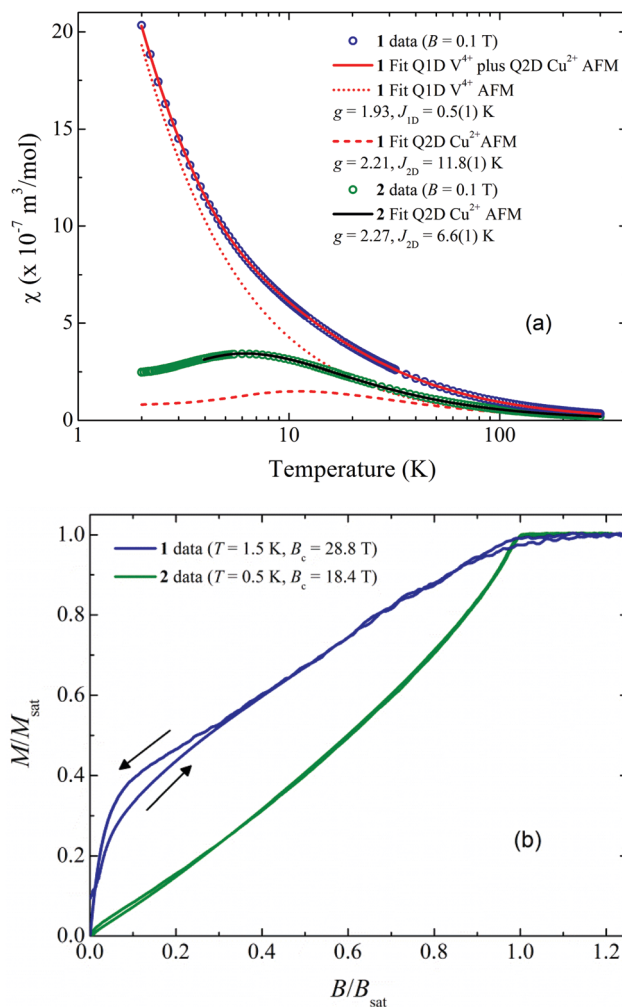

Fig. 2 (a) Magnetic susceptibility data (open symbols) for **1** and **2**. Solid lines represent theoretical fits as described in the text. (b) Pulsed-field magnetization data for **1** and **2** at low temperatures.

in Fig. 2a. At first glance, **1** appears to be paramagnetic without any anomalies that would have indicated a magnetic phase transition whereas **2** displays a broad maximum at 6 K, a feature typical of other quasi-2D coordination polymers including $Cu(ClO_4)_2(pyz)_2$[11] and $[Cu(HF_2)(pyz)_2]X$ (X = BF_4^-, PF_6^-, SbF_6^-, TaF_6^-) that show short-range spin correlations.[9–13] The lack of a maximum in $\chi(T)$ for **1** suggests that the additional fluctuating (*i.e.*, paramagnetic) V^{4+} spin likely masks this feature. Being that Ga^{3+} in **2** is a closed-shell cation, the expected magnetic lattice is quasi-2D and should yield the observed broad maximum in $\chi(T)$.

The crystal structures of **1** and **2** contain common 2D $[Cu(pyz)_2]^{2+}$ square lattices and, as such, the primary exchange interaction is governed by Cu–pyz–Cu pathways (J_{2D}). Electron-spin resonance experiments (see ESI†) confirm that the Cu^{2+} magnetic $d_{x^2-y^2}$ orbital lies in the 2D CuN_4 plane for both **1** and **2**. Considering an additional (albeit weak) exchange interaction along V–F–Cu–F–V (J_{1D}) in **1**, the $\chi(T)$ data may be described by an antiferromagnetic (AFM) Heisenberg $S = 1/2$ model ($\hat{H} = J\sum S_i \cdot S_j$) based on the sum of two components; a 2D quadratic lattice[14]

and orthogonal 1D chains.[15] For **2**, only the quadratic model was required. In Fig. 2a, the results of the least-squares fit give excellent reproducibility with the data for the following parameters; g_{Cu} = 2.21(1), g_V = 1.93(1), J_{2D} = 11.8(1) K, and J_{1D} = 0.5(1) K for **1** and g_{Cu} = 2.27(1) and J_{2D} = 6.6(1) K for **2**. The fitted Landé g-factors are average values and agree with the ESR-determined values.

Pulsed-field magnetization[16] data for **1** and **2** acquired up to 40 T and at T = 0.5 K are shown in Fig. 2b. The main difference exhibited by the two compounds is the low-field region below ∼10 T where **1** shows hysteresis between up- and down-field sweeps which is attributed to fluctuating V^{4+} moments. Above 10 T, the magnetization rises in a concave fashion which is indicative of low-dimensional spin interactions.[16] In contrast, **2** shows only a concave rise in the magnetization with a critical field (B_c) of 18.4 T (as determined by the midpoint of the gradient in dM/dB) which is substantially less than the 28.8 T critical field found in **1**. We can use these critical fields to independently deduce J_{2D} based on the simple relationship, $J_{2D} \approx g_{Cu}B_c/6.03$ T,[16] which gives 10.6(1) K (g_{Cu} = 2.21) and 6.8(1) K (g_{Cu} = 2.27) for **1** and **2**, respectively, of which the latter J_{2D} is in line with the value obtained from the fit of $\chi(T)$. We attribute the slight discrepancy between calculated and fitted J_{2D}'s for **1** as being due to the gradual approach to saturation resulting in a broadened transition.

The Cu–pyz–Cu magnetic interaction for **1** and **2** can be rationalized by superexchange *via* the σ-bond network containing adjacent Cu magnetic $d_{x^2-y^2}$ orbitals and lone-pair orbitals located on N-atoms. The weak interaction mediated along V–F–Cu–F–V is not surprising in that the spin-paired d_{z^2} orbital (of Cu) overlaps the p_z orbital of F ligands. Because F$^-$ has no practical π-acceptor character, any interaction along this pathway is likely facilitated by mixing of the Cu $d_{x^2-y^2}$ and d_{z^2} orbitals. In addition, the single V^{4+} electron resides in a π-type orbital (*i.e.*, d_{xy}, d_{xz}, or d_{yz}). Its overlap with $d_{x^2-y^2}$(Cu), although not zero by symmetry due to the relative orientations of the CuN_4F_2 and VF_6^{2-} octahedra, is predicted to be rather small.

Broken symmetry (BS) density-functional theoretical (DFT) calculations[17] were undertaken for **1** in order to corroborate this picture. Calculations were performed on dinuclear fragments of the experimental structure namely, *trans,trans*-[(pyz)$_3$CuF$_2$(μ-pyz)-CuF$_2$(pyz)$_3$] and *trans*-[(HF)Cu(pyz)$_4$(μ-F)VF$_5$]. In the latter case a proton was added to the terminal fluoride on copper in an optimized position with F_{Cu}–H of 1.18 Å in order for both fragments to have the same charge. The computed spin density distributions for the two fragments are shown in Fig. 3. The exchange coupling constants were calculated to be AFM (12.6 K) and FM (−0.29 K), supporting the experimental picture of a 2D magnetic structure with only very weak interactions along the V–F–Cu–F–V chains. Attempts to constrain $J > 0$ in the fit of $\chi(T)$ leads to g-factors different from those obtained by ESR. In either case $|J_{1D}|$ is consistently small and a spin polarization mechanism seemingly fails to explain the experimental result for Cu–F–V.

The presence of LRO in **1** and **2** was confirmed by muon-spin relaxation (μSR) measurements carried out at the STFC ISIS
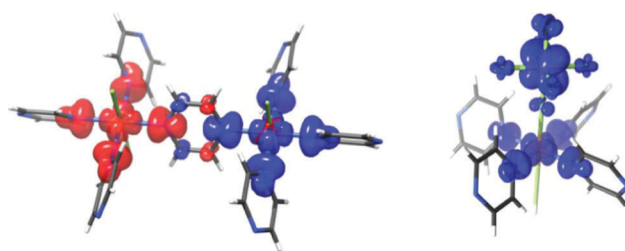

Fig. 3 DFT computed spin density distributions for the *trans,trans*-[(pyz)$_3$CuF$_2$(μ-pyz)CuF$_2$(pyz)$_3$] (left) and *trans*-[(HF)Cu(pyz)$_4$(μ-F)VF$_5$] (right). Isosurface values are ±0.00087 and ±0.002 Å^{-3}, respectively.

Facility, Rutherford-Appleton Laboratory (UK) using a sorption cryostat on the MuSR beamline and at the Swiss Muon Source, Paul Scherrer Institut (Switzerland) using the LTF instrument.

In data measured on **1** we observe oscillations in the muon polarization below 3.5 K at a single frequency. These oscillations reflect the coherent precession of muon spins about a local quasi-static B-field implying that the system is in a state of LRO. The precession frequency ν is plotted against T in Fig. 4. The frequency ν may be taken as an effective order parameter for the system, and is fitted to the phenomenological function $\nu(T) = \nu(0)(1 - (T/T_N)^\alpha)^\beta$. We obtain a fitted value for the critical temperature of T_N = 3.5(2) K and an exponent β = 0.33(3), the latter suggesting that fluctuations in this system have a three-dimensional character. The observed behavior of **1** is similar to other S = 1/2 Cu^{2+} molecular magnets studied previously[18] in both transition temperature and magnitude of internal field at the muon site. However, the oscillations observed for this system are significantly more damped than found in previous cases, likely caused by spatial or temporal fluctuations of magnetic moments on the V^{4+} ions. Data measured above 3.5 K show slow, heavily damped oscillations attributable to dipole–dipole interactions between muons and ^{19}F nuclei as observed previously in other fluorine-containing molecule-based magnets.[19]

In the data measured on **2** no well-resolved oscillations exist at any measured temperature down to 0.025 K, indicating a broader distribution of magnetic fields in **2** compared to **1**. However, there is a distinct change in shape of the muon spectra
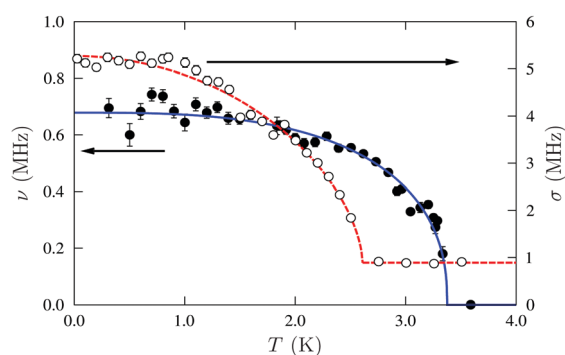

Fig. 4 Evolution of the muon spin precession frequency ν for **1** (filled circles) and the Gaussian relaxation rate σ for **2** (unfilled circles). The blue line denotes the fit described in the text; the red line is a guide to the eye.

below 2.6 K involving a sizeable increase in the Gaussian relaxation rate σ. This relaxation rate represents the width of the local field distribution experienced by the muon ensemble and is expected to scale with the magnitude of the average local field. The evolution of σ with temperature is also shown in Fig. 4 and closely resembles the expected order parameter behavior, decreasing as 2.6(1) K is approached from below. Taken together with the discontinuous decrease in the non-relaxing muon polarization above T_N (which often accompanies a magnetic ordering transition),[18] we conclude that **2** undergoes a transition to LRO below $T_N = 2.6(1)$ K.

The self-assembly of Cu^{2+} and MF_6^{n-} building blocks {M = V^{4+} (**1**) or Ga^{3+} (**2**)} leads to promising magnetic MOFs. Quasi-1D alternating chains of M–F–Cu–F–M are formed that are cross-linked by pyrazine ligands to form robust 3D frameworks. Water molecules fill interstitial sites in both compounds but additional H_3O^+ molecules are needed to balance charge in **2**. The magnetism of **1** and **2** is dominated by exchange interactions manifested by 2D $[Cu(pyz)_2]^{2+}$ square lattices albeit of differing strengths ($J_{2D} = 11.8$ and 6.6 K for **1** and **2**, respectively). Presently, the disparity in J_{2D} values cannot be rationalized as previous works have failed to establish magnetostructural correlations in related quasi-2D systems.[20] In **1**, the $S = 1/2$ V^{4+} moments continue to fluctuate down to 0.5 K but foster a weak interlayer magnetic interaction resulting in a higher T_N of 3.5 K compared to $T_N = 2.6$ K for **2**. Corresponding T_N/J ratios of 0.30 and 0.39 suggest enhanced low-dimensionality in **1** despite its higher T_N value. This may suggest the presence of additional symmetry-breaking terms in the spin Hamiltonian that are not presently considered.

Notes and references

§ Stoichiometric amounts of CuF_2, VF_4 and pyrazine were dissolved together in 48% HF(aq) to give a blue-green solution. Upon slow evaporation of the solvent overnight, X-ray quality blue prisms of **1** crystallized in high yield. Blue plates of **2** were obtained by the reaction of CuF_2, GaF_3, NH_4HF_2 and pyrazine in H_2O with slow evaporation of the solvent. Infrared spectroscopic data reveal the expected stretching and bending modes of H_2O, pyz and MF_6^{n-}. Further details of the SQUID, pulsed-field magnetization, and muon-spin relaxation measurements can be found in ref. 10 and 16.

1 *Magnetism: Molecules to Materials*, ed. J. S. Miller and M. Drillon, Wiley-VCH, Weinheim, 2002–2004, vol. 1–5, and references therein.
2 J. L. Fourquet, F. Plet, Y. Calage and R. de Pape, *J. Solid State Chem.*, 1987, **69**, 76–80.
3 A. B. Ali, M. T. Dang, J.-M. Greneche, A. Hemon-Ribaud, M. Leblanc and V. J. Maisonneuve, *J. Solid State Chem.*, 2007, **180**, 1911–1917.
4 D. W. Aldous, N. F. Stephens and P. Lightfoot, *Dalton Trans.*, 2007, 2271–2282.
5 T. Mahenthirarajah, Y. Li and P. Lightfoot, *Inorg. Chem.*, 2008, **47**, 9097–9102.
6 For a review, see: J. M. Herrera, A. Bachschmidt, F. Villain, A. Bleuzen, V. Marvaud, W. Wernsdorfer and M. Verdaguer, *Philos. Trans. R. Soc., A*, 2008, **366**, 127–138.
7 D. L. Reger, A. E. Pascui, M. D. Smith, J. Jezierska and A. Ozarowski, *Inorg. Chem.*, 2012, **51**, 11820–11836.
8 Crystallographic data for **1**: $C_8H_{16}N_4F_6O_4VCu$, $M = 460.73$, tetragonal, space group $P4/nbm$, $a = b = 9.7325(2)$, $c = 8.2154(1)$ Å, $U = 778.18(2)$ Å^3, $T = 100$ K, $Z = 2$, $\mu(MoK_\alpha) = 2.056$ mm^{-1}, 9707 reflections measured, 626 unique ($R_{int} = 0.0195$) which were used in all calculations. The final agreement factors were $R_1 = 0.0220$, w$R_2 = 0.0660$, GoF = 0.816. For **2**: $C_8H_{16}N_4F_6O_4GaCu$, $M = 479.50$, tetragonal, space group $P4/nbm$, $a = b = 9.7134(2)$, $c = 8.2415(1)$ Å, $U = 777.59(2)$ Å^3, $T = 100$ K, $Z = 2$, $\mu(MoK_\alpha) = 3.189$ mm^{-1}, 9957 reflections measured, 761 unique ($R_{int} = 0.0172$) which were used in all calculations. The final agreement factors were $R_1 = 0.0203$, w$R_2 = 0.0558$, GoF = 1.135.
9 J. L. Manson, M. M. Conner, J. A. Schlueter, T. Lancaster, S. J. Blundell, M. L. Brooks, F. L. Pratt, T. Papageorgiou, A. D. Bianchi, J. Wosnitza and M.-H. Whangbo, *Chem. Commun.*, 2006, 4894–4896.
10 J. L. Manson, J. A. Schlueter, K. A. Funk, H. I. Southerland, B. Twamley, T. Lancaster, S. J. Blundell, P. J. Baker, F. L. Pratt, J. Singleton, R. D. McDonald, P. A. Goddard, P. Sengupta, C. D. Batista, L. Ding, C. Lee, M.-H. Whangbo, I. Franke, S. Cox, C. Baines and D. Trial, *J. Am. Chem. Soc.*, 2009, **131**, 6733–6747.
11 F. M. Woodward, P. J. Gibson, G. B. Jameson, C. P. Landee, M. M. Turnbull and R. D. Willett, *Inorg. Chem.*, 2007, **46**, 4256–4266.
12 E. Čižmár, S. A. Zvyagin, R. Beyer, M. Uhlarz, M. Ozerov, Y. Skourski, J. L. Manson, J. A. Schlueter and J. Wosnitza, *Phys. Rev. B: Condens. Matter Mater. Phys.*, 2010, **81**, 064422.
13 J. L. Manson, J. A. Schlueter, R. D. McDonald and J. Singleton, *J. Low Temp. Phys.*, 2010, **159**, 15–18.
14 F. M. Woodward, A. S. Albrecht, C. M. Wynn, C. P. Landee and M. M. Turnbull, *Phys. Rev. B: Condens. Matter Mater. Phys.*, 2002, **65**, 144412.
15 A. Klümper and D. C. Johnston, *Phys. Rev. Lett.*, 2000, **84**, 4701.
16 P. A. Goddard, J. Singleton, P. Sengupta, R. D. McDonald, T. Lancaster, S. J. Blundell, F. L. Pratt, S. Cox, N. Harrison, J. L. Manson, H. I. Southerland and J. A. Schlueter, *New J. Phys.*, 2008, **10**, 083025.
17 The computational approach has been detailed previously: J. L. Manson, *et al.*, *Inorg. Chem.*, 2011, **50**, 5990–6009 and references therein.
18 A. J. Steele, T. Lancaster, S. J. Blundell, P. J. Baker, F. L. Pratt, C. Baines, M. M. Conner, H. I. Southerland and J. A. Schlueter, *Phys. Rev. B: Condens. Matter Mater. Phys.*, 2011, **84**, 064412.
19 T. Lancaster, S. J. Blundell, P. J. Baker, M. L. Brooks, W. Hayes, F. L. Pratt, J. L. Manson, M. M. Conner and J. A. Schlueter, *Phys. Rev. Lett.*, 2007, **99**, 267601.
20 (*a*) L. H. R. Dos Santos, A. Lanza, A. M. Barton, J. Brambleby, W. J. A. Blackmore, P. A. Goddard, F. Xiao, R. C. Williams, T. Lancaster, F. L. Pratt, S. J. Blundell, J. L. Manson and P. Macchi, *J. Am. Chem. Soc.*, 2016, **138**, 2280–2291; (*b*) S. Vela, J. Jornet-Somoza, M. M. Turnbull, R. Feyerherm, J. J. Novoa and M. Deumel, *Inorg. Chem.*, 2013, **52**, 12923–12932.